Computational Methods for Differential Equations
http://cmde.tabrizu.ac.ir
Vol. 4, No. 2, 2016, pp. 99-115

Biorthogonal cubic Hermite spline multiwavelets on the interval for solving the fractional optimal control problems

Elmira Ashpazzadeh
Department of Applied Mathematics,
Faculty of Mathematical Sciences,
University of Tabriz, Tabriz, Iran.
E-mail: e.ashpazzadeh@gmail.com

Mehrdad Lakestani*
Department of Applied Mathematics,
Faculty of Mathematical Sciences,
University of Tabriz, Tabriz, Iran.
E-mail: lakestani@tabrizu.ac.ir

Abstract In this paper, a new numerical method for solving fractional optimal control problems (FOCPs) is presented. The fractional derivative in the dynamic system is described in the Caputo sense. The method is based upon biorthogonal cubic Hermite spline multiwavelets approximations. The properties of biorthogonal multiwavelets are first given. The operational matrix of fractional Riemann-Lioville integration and multiplication are then utilized to reduce the given optimization problem to the system of algebraic equations. In order to save memory requirement and computational time, a threshold procedure is applied to obtain spare algebraic equations. Illustrative examples are provided to confirm the applicability of the new method.

Keywords. Caputo fractional derivative, Fractional order optimal control, Biorthogonal cubic Hermite spline multiwavelets.

2010 Mathematics Subject Classification. 65L05, 34K06, 34K28.

1. Introduction

In the present paper, we focus on optimal control problems with the quadratic performance index and the dynamic system with the Caputo fractional derivative as follows

$$Min\ J(x,u) = \frac{1}{2}\int_{t_0}^{t_1} [q(t)x^2(t) + r(t)u^2(t)]dt, \tag{1.1}$$

$${}_{t_0}^{C}D_t^{\alpha} x(t) = a(t)x(t) + b(t)u(t), \tag{1.2}$$

$$x(t_0) = x_0, \tag{1.3}$$

where $q(t) \geq 0$, $r(t) > 0$ and $b(t) \neq 0$. The behavior of many real-world physical phenomena is governed by fractional differential equations (FDEs) [24]. FDEs are generalizations of ordinary differential equations to an arbitrary (non-integer) order.

Received: 4 August 2016 ; Accepted: 8 November 2016.
* Corresponding author.

When these equations are used in conjunction with a performance index and a set of initial conditions, they lead to FOCPs. Fractional optimal control theory is a very new area in mathematics and the number of publications on this subject is limited.

Wavelet theory is a relatively new and an emerging area in mathematical research [20]. It has been applied in a wide range of engineering disciplines; particularly, wavelets are very successfully used in signal analysis for wave form representations and segmentations, time–frequency analysis and fast algorithms for easy implementation [13]. Wavelets permit the accurate representation of a variety of functions and operators. Moreover, wavelets establish a connection with fast numerical algorithms [12].

The main aim of this paper is to employ biorthogonal cubic Hermite spline multiwavelets on the interval $[0,1]$ as the interpolating functions to achieve high performance computations of FOCPs. Our method consists of reducing the FOCP to a set of algebraic equations. We approximate the fractional state rate ${}_{t_0}^{C}D_t^{\alpha}x(t)$ and control variable $u(t)$ with biorthogonal multiwavelets with unknown coefficients. Then the operational matrices of the Riemann–Liouville fractional integration and product are utilized to achieve a linear system of algebraic equation, instead of performance index (1.1) and dynamical system (1.2) in terms of unknown coefficients. Finally, the method of constrained extremum is applied which consists of adjoining the constraint equations derived from given dynamical system to the performance index by a set of undetermined Lagrange multipliers. As a result, the necessary conditions of optimality are derived as a system of algebraic equations in the unknown coefficients of ${}_{t_0}^{C}D_t^{\alpha}x(t)$ and $u(t)$ and the Lagrange multipliers. These coefficients are determined in such a way that the necessary conditions for extremization are imposed. Generally the use of biorthogonal cubic Hermite spline multiwavelets appears to be attractive since these functions possess several useful properties, such as small support, exact representation of polynomials to degree 3, Hermite interpolatory nature and the ability to represent functions at different levels of resolution, these considerations reduce the computations. The main advantage of the new method is that with the use of threshold procedure for biorthogonal multiwavelets, we obtain spare algebraic equation and this is computationally very attractive and reduces CPU time.
Some numerical simulations for FOCPs with Riemann–Liouville fractional derivative can be found in [4, 5, 11, 22, 26]. Also there exist numerical simulations for FOCPs with the Caputo fractional derivative such as [6, 7, 27], where the author has solved the problem by solving the Hamiltonian equations approximately. Lotfi et. al. [22] and Keshavarz et. al [18] have solved the linear quadratic FOCP directly without using Hamiltonian formula. Also we refer the interested reader in fractional optimization problems to see [1, 2, 3, 8, 9, 10, 11, 12, 14, 19, 21, 23] for some recent works in the subject.

The outline of this paper is as follows. In the next section, we describe some necessary basic definitions of the fractional calculus theory required for our subsequent development. In Section 3, we describe many desired properties of biorthogonal Hermite cubic spline multiwavelets on $[0,1]$. In Section 4, we apply biorthogonal multiwavelets on $[0,1]$ to solve equations (1.1)-(1.3). In Section 5, two example have been presented to demonstrate the accuracy of our proposed method, in comparison with the numerical solutions obtained by [18, 22]. Finally, Section 6 completes this paper with a brief conclusion. Note that we have computed the numerical results by MAPLE programming.

2. Basic definition on fractional calculus

We give some basic definitions and properties of the fractional calculus theory which are used further in this paper.

Definition 2.1. The Riemann–Liouville fractional integral of order $\alpha > 0$ of a function f is defined as follows [25]

$$ {}_0I_t^{\alpha} f(t) = \begin{cases} \dfrac{1}{\Gamma(\alpha)} \int_0^t (t-\tau)^{\alpha-1} f(\tau) d\tau, & \alpha > 0, \\ f(t), & \alpha = 0. \end{cases} $$

Definition 2.2. The Caputo fractional derivative of order $\alpha > 0$ of a function f is defined as follows

$$ {}_0^C D_t^{\alpha} f(t) = \begin{cases} \dfrac{1}{\Gamma(n-\alpha)} \int_0^t (t-\tau)^{n-\alpha-1} \dfrac{d^n}{d\tau^n} f(\tau) d\tau, & n-1 < \alpha < n, \\ f^{(n)}(t), & \alpha = n. \end{cases} $$

where n is a positive integer.

For Riemann–Liouville fractional integration and the Caputo fractional derivative we have the following properties [25].

(1) For real values of $\alpha > 0$, the Caputo fractional derivative provides the operation inverse to the Riemann–Liouville integration from the left

$$ {}_0^C D_t^{\alpha}\, {}_0I_t^{\alpha} f(t) = f(t), \quad \alpha > 0, f(t) \in C[0,1]. \tag{2.1} $$

(2) if $f(t) \in C^{\lceil \alpha \rceil}[0,1]$, then

$$ {}_0I_t^{\alpha}\, {}_0^C D_t^{\alpha} f(t) = f(t) - \sum_{j=0}^{\lceil \alpha \rceil - 1} \frac{t^j}{j!} \left(\frac{d^j}{dt^j} f \right)(0), \quad n-1 < \alpha \leq n, \tag{2.2} $$

where $C^{\lceil \alpha \rceil}[0,1]$ is the space of $\lceil \alpha \rceil$ times continuously differentiable functions.

3. Biorthogonal Hermite cubic spline multiwavelets

The widely used Hermite cubic splines $\phi = (\phi^1, \phi^2)^{\mathsf{T}}$ are given by [16]

$$ \begin{aligned} \phi^1(x) &:= (1 - 3x^2 - 2x^3)\chi_{[-1,0]} + (1 - 3x^2 + 2x^3)\chi_{[0,1]}, \\ \phi^2(x) &:= (x + 2x^2 + x^3)\chi_{[-1,0]} + (x - 2x^2 + x^3)\chi_{[0,1]}. \end{aligned} \tag{3.1} $$

Note that $\phi \in (C^1(\mathbb{R}))^2$ is a Hermite interpolant of order 1 satisfying

$$ \phi^1(k) = \boldsymbol{\delta}(k), \quad [\phi^1]'(k) = 0, \quad \phi^2(k) = 0, \quad [\phi^2]'(k) = \boldsymbol{\delta}(k) \quad \forall k \in \mathbb{Z}, \tag{3.2} $$

where $\boldsymbol{\delta}$ is the Dirac sequence such that $\boldsymbol{\delta}(0) = 1$ and $\boldsymbol{\delta}(k) = 0$ for all $k \in \mathbb{Z}\backslash\{0\}$. Moreover, the Hermite cubic spline vector-valued function ϕ is a refinable vector function satisfying

$$\phi(x) = 2\sum_{k\in\mathbb{Z}} a(k)\phi(2x-k), \qquad x \in \mathbb{R}, \tag{3.3}$$

with the following matrix-valued mask:

$$a(-1) = \begin{bmatrix} \frac{1}{4} & \frac{3}{8} \\ -\frac{1}{16} & -\frac{1}{16} \end{bmatrix}, \qquad a(0) = \begin{bmatrix} \frac{1}{2} & 0 \\ 0 & \frac{1}{4} \end{bmatrix}, \qquad a(1) = \begin{bmatrix} \frac{1}{4} & -\frac{3}{8} \\ \frac{1}{16} & -\frac{1}{16} \end{bmatrix} \tag{3.4}$$

and $a(k) = 0$ for all $k \in \mathbb{Z}\backslash\{-1, 0, 1\}$. Note that ϕ^1 and ϕ^2 have symmetry: $\phi^1(x) = \phi^1(-x)$ and $\phi^2(x) = -\phi^2(-x)$ for all $x \in \mathbb{R}$.
Define $\psi = (\psi_1, \psi_2)^T$ as follows [17]

$$\begin{aligned} \psi^1(x) &= \phi^1(2x) - \tfrac{1}{2}(\phi^1(2x+1) + \phi^1(2x-1)) - \tfrac{23}{12}(\phi^2(2x+1) - \phi^2(2x-1)), \\ \psi^2(x) &= \tfrac{37}{22}\phi^2(2x) + \tfrac{91}{88}(\phi^2(2x+1) + \phi^2(2x-1)) + \tfrac{1}{8}(\phi^1(2x+1) - \phi^1(2x-1)). \end{aligned} \tag{3.5}$$

Note that ϕ^1, ϕ^2 and ψ^1, ψ^2 are supported inside $[-1, 1]$. The functions ϕ^1, ψ^1 are symmetric about the origin, while ϕ^2, ψ^2 are antisymmetric about the origin. Moreover, both ψ^1, ψ^2 have at least order 2 vanishing moments. See Figure 1 for the graphs of the refinable vector function ϕ and wavelet vector function ψ.

FIGURE 1. The graphs of the biorthogonal wavelet $(\{\phi; \psi\})$ for $L_2(\mathbb{R})$, where $\phi = (\phi^1, \phi^2)^\mathsf{T}$ is the spline Hermite refinable interpolant and $\psi = (\psi^1, \psi^2)^\mathsf{T}$ is the wavelet vector function.

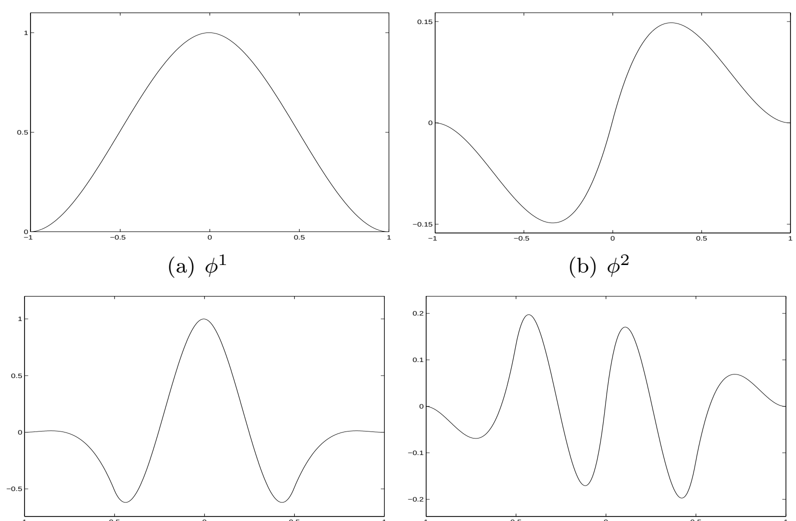

(a) ϕ^1 (b) ϕ^2

(c) ψ^1 (d) ψ^2

3.1. **Function Approximation.** In this section we consider the approximation properties of wavelet bases on the interval $[0,1]$. A Riesz wavelet basis $\mathscr{B}_{J_0,\mathsf{J}} = \vec{\Phi}_{J_0} \cup \cup_{j=J_0}^{\mathsf{J}-1} \vec{\Psi}_j$ for $L_2([0,1])$ is given by

$$\vec{\Phi}_j = \left[\sqrt{2}\phi^1_{2^j;0}|_{[0,1]}, \phi^1_{2^j;1}, \phi^2_{2^j;1}, \ldots, \phi^1_{2^j;2^j-1}, \phi^2_{2^j;2^j-1}, \sqrt{2}\phi^1_{2^j;2^j}|_{[0,1]}\right]^{\mathsf{T}}, \tag{3.6}$$

$$\vec{\Psi}_j = \left[\sqrt{2}\psi^1_{2^j;0}|_{[0,1]}, \psi^1_{2^j;1}, \psi^2_{2^j;1}, \ldots, \psi^1_{2^j;2^j-1}, \psi^2_{2^j;2^j-1}, \sqrt{2}\psi^1_{2^j;2^j}|_{[0,1]}\right]^{\mathsf{T}}. \tag{3.7}$$

Define $\mathscr{V}_j$ and $\mathscr{W}_j$ to be the linear spaces spanned by the entries of $\vec{\Phi}_j$ and $\vec{\Psi}_j$, respectively. For these spaces we have

$$\mathscr{V}_{j-1} \subseteq \mathscr{V}_j \quad \text{and} \quad \mathscr{V}_j = \mathscr{V}_{j-1} + \mathscr{W}_{j-1} = \mathscr{V}_{j_0} + \mathscr{W}_{j_0} + \cdots + \mathscr{W}_{j-1}, \qquad \forall\, 0 \le j_0 < j \in \mathbb{N},$$

where the above $+$ stands for a direct sum of finite dimensional spaces. Note that both the set formed by all the entries in $\vec{\Phi}_j$ and the set formed by all the entries in $\vec{\Phi}_{j_0}, \vec{\Psi}_{j_0}, \ldots, \vec{\Psi}_{j-1}$ are bases for the finite dimensional space $\mathscr{V}_j$.
A function $f(x)$ on $[0,1]$ may be represented by the corresponding multiwavelet functions as

$$f(x) \approx \mathbf{P}_{\mathsf{J}}\mathbf{f}(\mathbf{x}) = c^1_{J_0;0}\sqrt{2}\phi^1_{2^{J_0};0}|_{[0,1]} + c^1_{J_0;2^{J_0}}\sqrt{2}\phi^1_{2^{J_0};2^{J_0}}|_{[0,1]} + \sum_{\ell=1}^{2}\sum_{k=1}^{2^{J_0}-1} c^\ell_{J_0;k}\phi^\ell_{2^{J_0};k} +$$
$$\sum_{j=J_0}^{\mathsf{J}-1}\left(d^1_{j;0}\sqrt{2}\phi^1_{2^j;0}|_{[0,1]} + d^1_{j;2^j}\sqrt{2}\phi^1_{2^j;2^j}|_{[0,1]} + \sum_{\ell=1}^{2}\sum_{k=1}^{2^j-1} d^\ell_{j;k}\phi^\ell_{2^j;k}\right), \tag{3.8}$$

where

$$c^\ell_{J_0;k} = \int_0^1 f(x)\tilde{\phi}^\ell_{2^{J_0};k}(x)dx, \quad \ell = 1,2, \quad k = 0,\ldots,2^{J_0}, \tag{3.9}$$

$$d^\ell_{j;k} = \int_0^1 f(x)\tilde{\psi}^\ell_{2^j;k}(x)dx, \quad \ell = 1,2, \quad k = 0,\ldots,2^j, \quad j = J_0,\ldots,\mathsf{J}-1, \tag{3.10}$$

We refer to P_{J} as the projection to f onto $\mathscr{V}_{\mathsf{J}}$.

Theorem 3.1. *Suppose that a function $f : [0,1] \to \mathbb{R}$ is in $C^4[0,1]$. Then the operator P_J maps the function f into space V_J with error order as follows*

$$e_J(x) := |f(x) - P_J(x)| = O(2^{-J}).$$

Proof. See [14]. □

Here, to avoid computing of the integral obtained in Eq. (3.9) and Eq. (3.10) we present the translation matrix G by considering

$$\mathscr{B}_{J_0,\mathsf{J}}(x) = G\Phi_{\mathsf{J}}(x), \tag{3.11}$$

where G is a $(M \times M)$ matrix with $M = 2^{\mathsf{J}+1}$, which can be calculated as follows. Using Eq. (3.3) gives

$$\Phi_k = \beta_k\Phi_{k+1}, \tag{3.12}$$

where $\beta_k,\ k = J_0,\dots,\mathsf{J}-1$ is a $(2^{k+1}\times 2^{k+2})$ matrix, and the entries of β_k are the coefficients of the mask matrices given in (3.4). From (3.5) we have

$$\Psi_k = \theta_k \Phi_{k+1}, \tag{3.13}$$

where $\theta_k,\ k = J_0,\dots,\mathsf{J}-1$ is a $(2^{k+1}\times 2^{k+2})$ matrix, and the entries of θ_k are the coefficients in the refinement equation for multiwavelet given in (3.4). Using Eq. (3.12) and Eq. (3.13) we get

$$G = \begin{bmatrix} \beta_{J_0+1}\times\beta_{J_0+2}\times\dots\times\beta_{\mathsf{J}} \\ ---------- \\ \theta_{J_0+1}\times\beta_{J_0+2}\times\dots\times\beta_{\mathsf{J}} \\ ---------- \\ \vdots \\ \theta_{\mathsf{J}-2}\times\beta_{\mathsf{J}-1}\times\times\beta_{\mathsf{J}} \\ ---------- \\ \theta_{\mathsf{J}-1}\times\beta_{\mathsf{J}} \\ ---------- \\ \theta_{\mathsf{J}} \end{bmatrix}. \tag{3.14}$$

3.2. **The Operational matrix of integration.** Using the Hermite interpolation property of ϕ, we can approximate the functions $\int_0^t \phi^i(2^{\mathsf{J}}x-l)dx$ for $l=1,\dots 2^{\mathsf{J}}-1$ and $\int_0^t \sqrt{2}\phi^1(2^{\mathsf{J}}x-l')|_{[0,1]}dx$ for $l'=0,2^{\mathsf{J}}$ as follows

$$\int_0^t \phi^i(2^{\mathsf{J}}x-l)dx = \sum_{k=1}^{2^{\mathsf{J}}-1}\left[\left(\int_0^{k/2^{\mathsf{J}}}\phi^i(2^{\mathsf{J}}x-l)dx\right)\phi^1_{2^{\mathsf{J}};k}(t)+\tfrac{1}{2^{\mathsf{J}}}\phi^i(k-l)\phi^2_{2^{\mathsf{J}};k}(t)\right]+ \\ \tfrac{1}{\sqrt{2}}\left(\int_0^1\phi^1(2^{\mathsf{J}}x-2^{\mathsf{J}})|_{[0,1]}dx\right)\sqrt{2}\phi^1_{2^{\mathsf{J}};2^{\mathsf{J}}}(t)|_{[0,1]},\quad i=1,\ 2,\quad l=1,\dots,2^{\mathsf{J}}-1, \tag{3.15}$$

$$\int_0^t \sqrt{2}\phi^1(2^{\mathsf{J}}x-l')|_{[0,1]}dx = \\ \sum_{k=1}^{2^{\mathsf{J}}-1}\left[\left(\sqrt{2}\int_0^{k/2^{\mathsf{J}}}\phi^i(2^{\mathsf{J}}x-l')dx\right)\phi^1_{2^{\mathsf{J}};k}(t)+\tfrac{\sqrt{2}}{2^{\mathsf{J}}}\phi^i(k-l')\phi^2_{2^{\mathsf{J}};k}(t)\right]+ \\ \left(\int_0^1\phi^1(2^{\mathsf{J}}x-2^{\mathsf{J}})|_{[0,1]}dx\right)\sqrt{2}\phi^1_{2^{\mathsf{J}};2^{\mathsf{J}}}(t)|_{[0,1]},\quad l'=0,\ 2^{\mathsf{J}}. \tag{3.16}$$

Then, the integration of vector $\vec{\Phi}_{\mathsf{J}}(x)$ given in (3.6) can be expressed as

$$\int_0^t \vec{\Phi}_{\mathsf{J}}(x)dx \approx I_1\vec{\Phi}_{\mathsf{J}}(x), \tag{3.17}$$

where I_1 is a $M \times M$ operational matrix of ingration. It can be shown that

$$I_1 = \frac{1}{2^{\mathsf{J}}}\begin{bmatrix} 0 & L & L & \cdots & \cdots & L & \frac{1}{2} \\ & H & S & \cdots & \cdots & S & L \\ & & H & S & \cdots & S & L \\ & & & \ddots & \ddots & \vdots & \vdots \\ & & & & H & S & \vdots \\ & & & & & H & L \\ & & & & & & \frac{1}{2} \end{bmatrix}, \tag{3.18}$$

$$H = \begin{bmatrix} \frac{1}{2} & 1 \\ -\frac{1}{12} & 0 \end{bmatrix}, \quad S = \begin{bmatrix} 1 & 0 \\ 0 & 0 \end{bmatrix}, \quad L = \begin{bmatrix} \frac{1}{2}\sqrt{2} & 0 \end{bmatrix}.$$

3.3. **The Operational matrix of fractional integration.** The Riemann–Liouville fractional integration of the vector given in Eq. (3.6) can be expressed by

$${}_0I_t^{\alpha}\vec{\Phi}_{\mathsf{J}}(x) \approx \mathrm{I}_{\alpha}\vec{\Phi}_{\mathsf{J}}(x), \tag{3.19}$$

where I_{α} is the $M \times M$ Riemann-Liouville fractional operational matrix of integration for Hermite cubic splines.

Using a similar method given in the last subsection, this matrix can be determined as follows

$$I_{\alpha} = \begin{bmatrix} 0 & \underline{\Omega} & \Omega_1 & \cdots & \cdots & \Omega_{2^{\mathsf{J}}-2} & \overline{\Omega} \\ & \Upsilon & \Lambda_1 & \Lambda_2 & \cdots & \Lambda_{2^{\mathsf{J}}-2} & \Delta_1 \\ & & \Upsilon & \Lambda_1 & \cdots & \Lambda_{2^{\mathsf{J}}-3} & \Delta_2 \\ & & & \ddots & \ddots & \vdots & \vdots \\ & & & & \Upsilon & \Lambda_1 & \vdots \\ & & & & & \Upsilon & \Delta_{2^{\mathsf{J}}-1} \\ & & & & & & \underline{\Delta} \end{bmatrix}, \tag{3.20}$$

where

$$\underline{\Omega} = 2^{-\mathsf{J}\alpha+\frac{1}{2}}\begin{bmatrix} \frac{\alpha(\alpha^2+6\alpha+5)}{\Gamma(\alpha+4)} & \frac{\alpha(\alpha^2+3\alpha-4)}{\Gamma(\alpha+3)} \end{bmatrix},$$

$$\Omega_{i-1} = 2^{-\mathsf{J}\alpha+\frac{1}{2}}\begin{bmatrix} \eta_{1,1}^{i-1} & \eta_{1,2}^{i-1} \end{bmatrix}, \quad i = 2\dots,2^{\mathsf{J}}-1,$$

$$\eta_{1,1}^{i-1} := -\frac{2^{-\mathsf{J}\alpha+\frac{1}{2}}}{\Gamma(\alpha+4)}[i^{\alpha}(-12i^3+(6\alpha+18)i^2-\alpha^3-6\alpha^2-11\alpha-6)+ \\ (i-1)^{\alpha}(12i^3+(6\alpha-18)i^2-12\alpha i+6\alpha+6)],$$

$$\eta_{1,2}^{i-1} := -\frac{2^{-\mathsf{J}\alpha+\frac{1}{2}}}{\Gamma(\alpha+4)i}[i^{\alpha}(12(\alpha+3)i^3-6(6+\alpha^2+5\alpha)i^2+11\alpha^2+6\alpha^3+6\alpha+\alpha^4)+ \\ (i-1)^{\alpha}(-12(\alpha+3)i^3-6(\alpha^2+\alpha-6)+6(\alpha^2+3\alpha)i)],$$

$$\Upsilon = 2^{-\mathsf{J}\alpha+1}\begin{bmatrix} \frac{3(\alpha+1)}{\Gamma(\alpha+4)} & \frac{3\alpha}{\Gamma(\alpha+3)} \\ -\frac{\alpha}{\Gamma(\alpha+4)} & -\frac{(\alpha-1)}{\Gamma(\alpha+3)} \end{bmatrix},$$

$$\Lambda_1 = 2^{-\mathsf{J}\alpha+2}\begin{bmatrix} \frac{6(2^{\alpha}(\alpha-1)+1)}{\Gamma(\alpha+4)} & \frac{3(2^{\alpha}(\alpha-2)+2)}{\Gamma(\alpha+3)} \\ -\frac{2(2^{\alpha}(\alpha-3)+\alpha+3)}{\Gamma(\alpha+4)} & -\frac{(2^{\alpha}(\alpha-4)+2\alpha+4)}{\Gamma(\alpha+3)} \end{bmatrix},$$

$$\Lambda_i = \begin{bmatrix} \lambda^i_{1,1} & \lambda^i_{1,2} \\ \lambda^i_{2,1} & \lambda^i_{2,2} \end{bmatrix}, \qquad i = 1,\ldots,2^{\mathsf{J}}-2,$$

$$\lambda^i_{1,1} := -\frac{6\times 2^{(-\mathsf{J}\alpha)}}{\Gamma(\alpha+4)}[i^{\alpha+2}(2i-(\alpha+3)) + (i-1)^{\alpha}(-4i^3+2i^2-12i+4) + (i-2)^{\alpha}(2i^3+(\alpha-9)i^2-4(\alpha-3)i+4\alpha-4)],$$

$$\lambda^i_{1,2} := -\frac{6\times 2^{(-\mathsf{J}\alpha)}}{\Gamma(\alpha+3)}\left[i^{\alpha}(2i^2-(\alpha+2)i) + (i-1)^{\alpha}(4i^2+8i-4) + (i-2)^{\alpha}(2i^2+(\alpha-6)i-2\alpha+4)\right],$$

$$\lambda^i_{2,1} := -\frac{2^{(\mathsf{J}\alpha+1)}}{\Gamma(\alpha+4)}[i^{\alpha+2}(-3i+\alpha+3) + (i-1)^{\alpha}((12+4\alpha)i^2-8i(\alpha+3)+4\alpha+12) + (i-2)^{\alpha}(3i^3-(15-\alpha)i^2-4(\alpha-6)i+4\alpha-12)],$$

$$\lambda^i_{2,2} := -\frac{2^{(\mathsf{J}\alpha+1)}}{\Gamma(\alpha+3)}[i^{\alpha}(-3i^2+(\alpha+2)i) + (i-1)^{\alpha}((8+4\alpha)i-8-4\alpha) + (i-2)^{\alpha}(3i^2+(\alpha-10)i-2\alpha+8)],$$

$$\underline{\Delta} := \frac{6\times 2^{-\mathsf{J}\alpha}(\alpha+1)}{\Gamma(\alpha+4)},$$

$$\overline{\Omega} := \frac{1}{\Gamma(\alpha+4)}[(1-2^{-\mathsf{J}})^{\alpha}(-12\times 2^{3\mathsf{J}} + (18-6\alpha)2^{2\mathsf{J}} + 12\alpha\times 2^{\mathsf{J}} - 6\alpha - 6) + 12\times 2^{3\mathsf{J}} - (18+6\alpha)\times 2^{2\mathsf{J}} + \alpha^3 + 6\alpha^2 + 11\alpha + 6],$$

Now, for simplicity without loss of generality in operational matrix of integration given in (3.20), we consider the matrices $\Delta_i,\ i = 1,\ldots,2^{\mathsf{J}}-1$ for case $\mathsf{J} = 2$. It can be shown that

$$\Delta_i = \begin{bmatrix} \mu^i_{1,1} & \mu^i_{1,2} \end{bmatrix}, \qquad i = 1,\ldots,2^{\mathsf{J}}-1,$$

$$
\begin{aligned}
\mu^i_{1,1} :=& -\frac{3\sqrt{2}}{\Gamma(\alpha+4)}[(\tfrac{3}{4}-\tfrac{1}{4}i)^{\alpha}(-2i^3+(\alpha+21)i^2-6(\alpha+12)i+9\alpha+81)+ \\
& (1-\tfrac{1}{4}i)^{\alpha}(4i^3-48i^2+192i-256)+ \\
& (\tfrac{5}{4}-\tfrac{1}{4}i)^{\alpha}(-2i^3+(27-\alpha)i^2-10(12-\alpha)i-25\alpha+175)], \\
\mu^i_{1,2} :=& -\frac{\sqrt{2}}{\Gamma(\alpha+4)}[(\tfrac{3}{4}-\tfrac{1}{4}i)^{\alpha}(-3i^3+(\alpha+30)i^2-(6\alpha+99)i+9\alpha+108)+ \\
& (1-\tfrac{1}{4}i)^{\alpha}(4(\alpha+3)i^2-32(\alpha+3)i+192+64\alpha)+ \\
& (\tfrac{5}{4}-\tfrac{1}{4}i)^{\alpha}(3i^3+(\alpha-42)i^2+(-10\alpha+195)i+25\alpha-300)].
\end{aligned}
$$

3.4. **The operational matrix of product.** The following property of the product of two multiscaling function vectors will also be used. Let

$$\vec{\Phi}_{\mathsf{J}}(x)\vec{\Phi}^{\mathsf{T}}_{\mathsf{J}}(x)Z = \tilde{Z}\vec{\Phi}_{\mathsf{J}}(x), \tag{3.21}$$

where

$$Z = \left[z^1_{\mathsf{J};0}, z^1_{\mathsf{J};1}, z^2_{\mathsf{J};1}, \ldots, z^1_{\mathsf{J};2^{\mathsf{J}}-1}, z^2_{\mathsf{J};2^{\mathsf{J}}-1}, z^1_{\mathsf{J};2^{\mathsf{J}}}\right]^{\mathsf{T}},$$

is an $M \times 1$ vector, and $\tilde{Z}$ is a $M \times M$ operational matrix of product given by

$$\tilde{Z} = \begin{bmatrix}
\sqrt{2}z^1_{J;0} & & & & & & & & \\
& z^1_{\mathsf{J};1} & z^2_{J;1} & & & & & & \\
& & z^1_{\mathsf{J};1} & & & & & & \\
& & & z^1_{\mathsf{J};2} & z^2_{\mathsf{J};2} & & & & \\
& & & & z^1_{\mathsf{J};2} & & & & \\
& & & & & \ddots & & & \\
& & & & & & z^1_{\mathsf{J};2^{\mathsf{J}}-1} & z^1_{\mathsf{J};2^{\mathsf{J}}-1} & \\
& & & & & & & z^2_{J;2^J-1} & \\
& & & & & & & & \sqrt{2}z^1_{\mathsf{J};2^{\mathsf{J}}}
\end{bmatrix}. \tag{3.22}$$

4. Solving the fractional optimal control problems

In this section, we consider the FOCP given by

$$
\begin{aligned}
& \text{Min } J(x,u) = \frac{1}{2}\int_0^1 [q(t)x^2(t) + r(t)u^2(t)]dt, && (4.1) \\
& {}^C_0D^{\alpha}_t x(t) = a(t)x(t) + b(t)u(t), && (4.2) \\
& x(0) = x_0. && (4.3)
\end{aligned}
$$

The fractional state rate ${}^C_0D^{\alpha}_t x(t)$ and control variable $u(t)$ can be approximated by biorthogonal multiwavelets as

$$
\begin{aligned}
& {}^C_0D^{\alpha}_0 x(t) \approx X^{\mathsf{T}}\vec{\Phi}_{\mathsf{J}}(t), && (4.4) \\
& u(t) \approx U^{\mathsf{T}}\vec{\Phi}_{\mathsf{J}}(t), && (4.5)
\end{aligned}
$$

where X and U are unknown $M \times 1$ vectors. Similarly we have

$$x_0 \approx X_0^{\mathsf{T}}\vec{\Phi}_{\mathsf{J}}(t), \tag{4.6}$$

where X_0 is $M\times 1$ vector of order $M\times 1$. Using Eqs. (2.2) and (3.19), $x(t)$ can be represented as

$$x(t) =_0 I_t^{\alpha}\ {}_0^C D_t^{\alpha} x(t) + x(0) \approx (X^{\mathsf{T}}\mathrm{I}_{\alpha} + X_0^{\mathsf{T}})\vec{\Phi}_{\mathrm{J}}(t). \tag{4.7}$$

We now expand $a(t)$, $b(t)$, $q(t)$ and $r(t)$ by biorthogonal multiwavelets as

$$a(t) \approx A^{\mathsf{T}}\vec{\Phi}_{\mathrm{J}}(t), \qquad b(t) \approx B^{\mathsf{T}}\vec{\Phi}_{\mathrm{J}}(t), \tag{4.8}$$

$$q(t) \approx Q^{\mathsf{T}}\vec{\Phi}_{\mathrm{J}}(t), \qquad r(t) \approx R^{\mathsf{T}}\vec{\Phi}_{\mathrm{J}}(t), \tag{4.9}$$

where A, B, Q and R are known vectors of order $M\times 1$. Then we have

$$a(t)x(t) \approx (X^{\mathsf{T}}\mathrm{I}_{\alpha} + X_0^{\mathsf{T}})\vec{\Phi}_{\mathrm{J}}(t)\vec{\Phi}_{\mathrm{J}}^{\mathsf{T}}(t)A \approx (X^{\mathsf{T}}\mathrm{I}_{\alpha} + X_0^{\mathsf{T}})\tilde{A}\vec{\Phi}_{\mathrm{J}}(t), \tag{4.10}$$

$$b(t)u(t) \approx U^{\mathsf{T}}\vec{\Phi}_{\mathrm{J}}(t)\vec{\Phi}_{\mathrm{J}}^{\mathsf{T}}(t)B \approx U^{\mathsf{T}}\tilde{B}\vec{\Phi}_{\mathrm{J}}(t), \tag{4.11}$$

where $\tilde{A}$ and $\tilde{B}$ can be calculated similarly to matrix $\tilde{Z}$ in Eq. (3.22).
By using Eqs. (4.5), (4.7) and (4.9), the performance index J can be approximated as

$$J[X,U] \approx \frac{1}{2}\int_0^1 [(X^{\mathsf{T}}\mathrm{I}_{\alpha} + X_0^{\mathsf{T}})\vec{\Phi}_{\mathrm{J}}(t).\vec{\Phi}_{\mathrm{J}}^{\mathsf{T}}(t)Q.\vec{\Phi}_{\mathrm{J}}^{\mathsf{T}}(t)(X^{\mathsf{T}}\mathrm{I}_{\alpha} + X_0^{\mathsf{T}}) + U^{\mathsf{T}}\vec{\Phi}_{\mathrm{J}}(t).\vec{\Phi}_{\mathrm{J}}^{\mathsf{T}}(t)R.\vec{\Phi}_{\mathrm{J}}^{\mathsf{T}}(t)U]dt$$

$$= \frac{1}{2}\Big((X^{\mathsf{T}}\mathrm{I}_{\alpha} + X_0^{\mathsf{T}})\tilde{Q}P(X^{\mathsf{T}}\mathrm{I}_{\alpha} + X_0^{\mathsf{T}}) + U^{\mathsf{T}}\tilde{R}PU\Big),$$

where $P = \int_0^1 \vec{\Phi}_{\mathrm{J}}^{\mathsf{T}}(t)\vec{\Phi}_{\mathrm{J}}(t)dt$.
Also, using Eqs. (4.4), (4.10) and (4.11), the dynamical system (4.2) can be approximated as

$$X^{\mathsf{T}}\vec{\Phi}_{\mathrm{J}}(t) - (X^{\mathsf{T}}\mathrm{I}_{\alpha} + X_0^{\mathsf{T}})\tilde{A}\vec{\Phi}_{\mathrm{J}}(t) - U^{\mathsf{T}}\tilde{B}\vec{\Phi}_{\mathrm{J}}(t) = 0. \tag{4.12}$$

Because of the independency of entries of vector $\vec{\Phi}_{\mathrm{J}}(t)$, we get

$$X^{\mathsf{T}} - (X^{\mathsf{T}}\mathrm{I}_{\alpha} + X_0^{\mathsf{T}})\tilde{A} - U^{\mathsf{T}}\tilde{B} = 0. \tag{4.13}$$

For simplicity, the above equation summarized as

$$\left[\begin{array}{cc} (I - \tilde{A}^{\mathsf{T}}{\mathrm{I}_{\alpha}}^{\mathsf{T}}) & -\tilde{B}^{\mathsf{T}} \end{array}\right].\left[\begin{array}{c} X \\ U \end{array}\right] + \tilde{A}^{\mathsf{T}}X_0 = 0, \tag{4.14}$$

in which I is a Identity matrix of order $M\times M$.
In order to solving described problem with the biorthogonal multiwavelets , it's enough to replace the basis vector $\vec{\Phi}_{\mathrm{J}}(t)$ by $G^{-1}\mathscr{B}_{J_0,\mathrm{J}}(t)$ in Eq (4.12). Therefore we obtain the last equation as the following form

$$\left[\begin{array}{cc} (G^{-\mathsf{T}} + G^{-\mathsf{T}}\tilde{A}^{\mathsf{T}}{\mathrm{I}_{\alpha}}^{\mathsf{T}}) & G^{-\mathsf{T}}\tilde{B}^{\mathsf{T}} \end{array}\right].\left[\begin{array}{c} X \\ U \end{array}\right] + G^{-\mathsf{T}}\tilde{A}^{\mathsf{T}}X_0 = 0. \tag{4.15}$$

Now, assume that

$$\mathcal{J}^*[X,U,\lambda] = \mathcal{J}[X,U] + \lambda[X^{\mathsf{T}} - (X^{\mathsf{T}}\mathrm{I}_{\alpha} + X_0^{\mathsf{T}})\tilde{A} - U^{\mathsf{T}}\tilde{B}],$$

where the vector λ represents the unknown Lagrange multiplier. Finally the necessary conditions for extremum are

$$\frac{\partial\mathcal{J}^*[X,U,\lambda]}{\partial X} = 0, \qquad \frac{\partial\mathcal{J}^*[X,U,\lambda]}{\partial U} = 0, \qquad \frac{\partial\mathcal{J}^*[X,U,\lambda]}{\partial\lambda} = 0. \tag{4.16}$$

The above equation are nonlinear equations then can be solved for X, U and λ using the Newton's iteration method. After solving Eqs. (4.16), the approximate values of $u(t)$ and $x(t)$ can be determined form (4.5) and (4.7).

5. Illustrative examples

We applied the method presented in Section 4 and solved some examples to support our theoretical discussion. In order to save memory requirement and computation time, a threshold procedure is applied to obtain algebraic equations. In other words, we will investigate the performance of the present method by concerning the sparseness of resulted matrix equation through the numerical experiments. For this propose for thresholding parameter ε, the matrix sparsity (S_ε), is defined in [15] as

$$S_\varepsilon = \frac{N_0 - N_\varepsilon}{N_0} \times 100\%,$$

where N_0 is the total number of elements and N_ε is the number of elements remaining after thresholding.

Example 1. Consider the following time-invariant problem [18, 22]

$$\text{Min } J(x,u) = \int_0^1 [x^2(t) + u^2(t)]dt,$$

subject to the system dynamics

$$D_t^\alpha x(t) = -x(t) + u(t),$$

with initial condition

$$x(0) = 1.$$

Our aim is to find $u(t)$ which minimizes the performance index J. For this problem we have the exact solution in the case of $\alpha = 1$ as follows [1]

$$\begin{aligned} x(t) &= \cosh(\sqrt{2}t) + \beta \sinh(\sqrt{2}t), \\ u(t) &= (1+\sqrt{2}\beta)\cosh(\sqrt{2}t) + (\sqrt{2}+\beta)\sinh(\sqrt{2}t), \\ \beta &= -\frac{\cosh(\sqrt{2}) + \sqrt{2}\sinh(\sqrt{2})}{\sqrt{2}\cosh(\sqrt{2}) + \sinh(\sqrt{2})} \simeq -0.98, \end{aligned}$$

Not that the minimum value of performance index is $J = 0.192909$.

Using the method presented in the previous section, the results for Example 1, are reported in Tables I and II and Figures 2, 3 and 4. In Table I. we compare the absolute error of the state variable $x(t)$ when $\alpha = 1$ with the results obtained in [18, 22] for $\mathsf{J} = 6,\ 7,\ 8$. It is seen from Table I, the approximate values of the state variable $x(t)$ converge to the exact solution with increase of J. In Figure 2, we demonstrate the approximation of the state $x(t)$ and control $u(t)$ for different values of α together with the exact solution for $\alpha = 1$. Also we show that when α tend to 1, the approximate solutions for both state and control variables tend to the exact solutions for $\alpha = 1$. The graphs of state variable $x(t)$ and control variable $u(t)$ for $\alpha = 0.8$ and $\mathsf{J} = 7,\ 8$ are plotted in Figure 3, It is obvious that with increase in the number of the biorthogonal wavelet basis, the approximate values of $x(t)$ and $u(t)$ converge to the exact solutions. Table II, reports the sparsity and minimum value of J when $\alpha = 1$ for different values of thresholding parameter. Also Figure 4, shows the plot of the matrix elements for $\mathsf{J} = 7$ after thresolding.

FIGURE 2. Approximate state and control variables for $\mathsf{J} = 7$ and $\alpha = 0.8, 0.9, .099, 1$ and exact solution for $\alpha = 1$, Example 1.

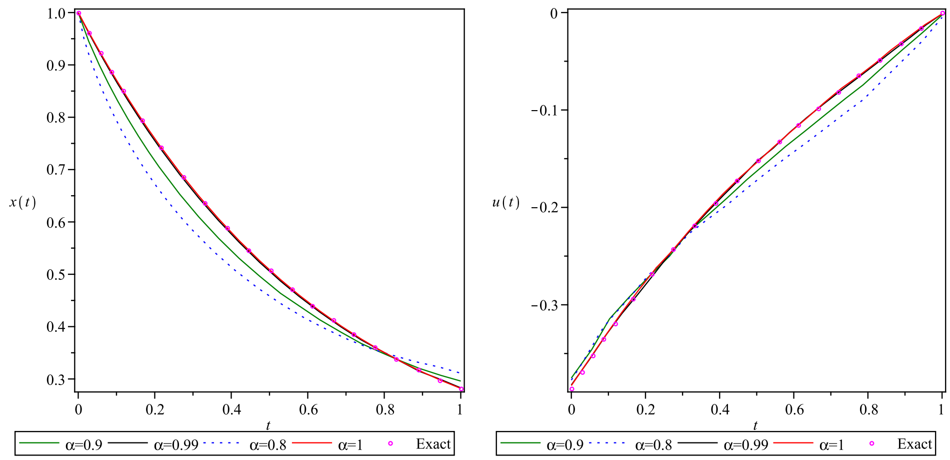

Table I. Absolute error of $x(t)$ with comparison to Refs, [18, 22].

t	Legendre basis [22] M = 4	Legendre basis [22] M = 5	Bernollin basis [18] M = 4	Bernollin basis [18] M = 5	Biorthogonal Multiwavelet J = 6	Biorthogonal Multiwavelet J = 7	Biorthogonal Multiwavelet J = 8
0	8.99×10^{-5}	6.25×10^{-6}	8.99×10^{-5}	6.25×10^{-6}	0.0	0.0	0.0
0.1	4.77×10^{-5}	1.34×10^{-5}	3.67×10^{-5}	2.39×10^{-6}	2.05×10^{-5}	5.07×10^{-6}	1.26×10^{-6}
0.2	3.25×10^{-5}	2.12×10^{-5}	1.01×10^{-5}	1.21×10^{-6}	1.67×10^{-5}	4.14×10^{-6}	1.03×10^{-6}
0.3	7.74×10^{-5}	3.24×10^{-5}	2.65×10^{-5}	1.72×10^{-6}	1.36×10^{-5}	3.36×10^{-6}	8.35×10^{-7}
0.4	2.13×10^{-5}	4.73×10^{-5}	1.53×10^{-5}	6.82×10^{-7}	1.09×10^{-6}	2.69×10^{-6}	6.68×10^{-7}
0.5	6.43×10^{-5}	6.20×10^{-5}	4.23×10^{-6}	1.93×10^{-6}	8.54×10^{-6}	2.11×10^{-6}	5.23×10^{-7}
0.6	1.03×10^{-4}	7.49×10^{-5}	2.91×10^{-5}	3.11×10^{-7}	6.54×10^{-6}	1.60×10^{-6}	3.99×10^{-7}
0.7	1.12×10^{-4}	8.88×10^{-5}	2.41×10^{-5}	1.90×10^{-6}	4.75×10^{-6}	1.17×10^{-6}	2.90×10^{-7}
0.8	9.14×10^{-5}	1.07×10^{-5}	1.73×10^{-5}	9.17×10^{-7}	3.24×10^{-6}	7.87×10^{-7}	1.94×10^{-7}
0.9	9.41×10^{-5}	1.31×10^{-5}	3.46×10^{-5}	2.49×10^{-6}	1.84×10^{-6}	4.44×10^{-7}	1.09×10^{-7}

Table II. Estimated values for J after thresholding, Example 1.

	Thresholding parameter (ε)	Sparsity (S_ε)	J
$\mathsf{J} = 6$	0	0%	0.192909
	10^{-4}	76.58%	0.192921
	10^{-3}	79.20%	0.192924
	10^{-2}	84.46%	0.189937
$\mathsf{J} = 7$	0	0%	0.192909
	10^{-4}	85.99%	0.192912
	10^{-3}	87.96%	0.192999
	10^{-2}	91.36%	0.192815

Example 2. consider the following time-varying problem [18, 22]. Find the control $u(t)$, which minimizes the performance index J

$$\text{Min } J(x,u) = \int_0^1 [x^2(t) + u^2(t)]dt,$$

FIGURE 3. Comparison of state $x(t)$ (left) and control $u(t)$ (right) for $\alpha = 0.8$ with $\mathsf{J} = 7,\ 8$, Example 1.

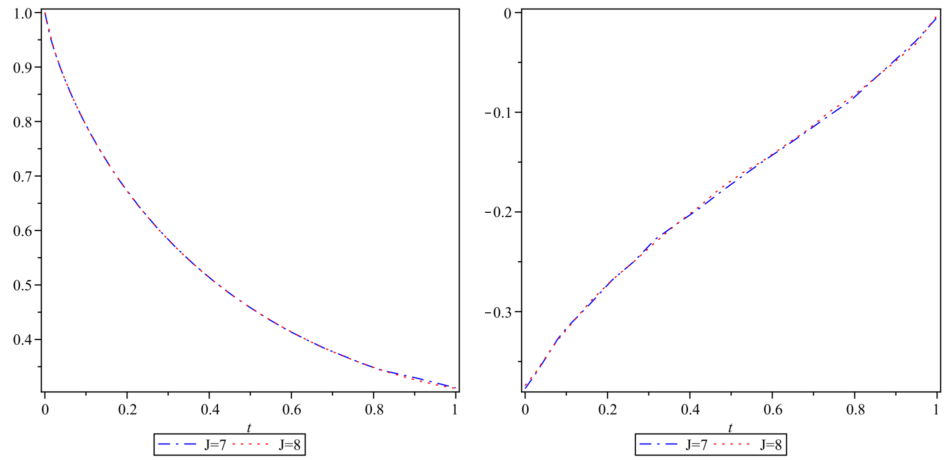

FIGURE 4. Plots of sparse matrices after thresholding with $\varepsilon = 10^{-3}$ (left) and $\varepsilon = 10^{-2}$ (right) for $\mathsf{J} = 7$, Example 1.

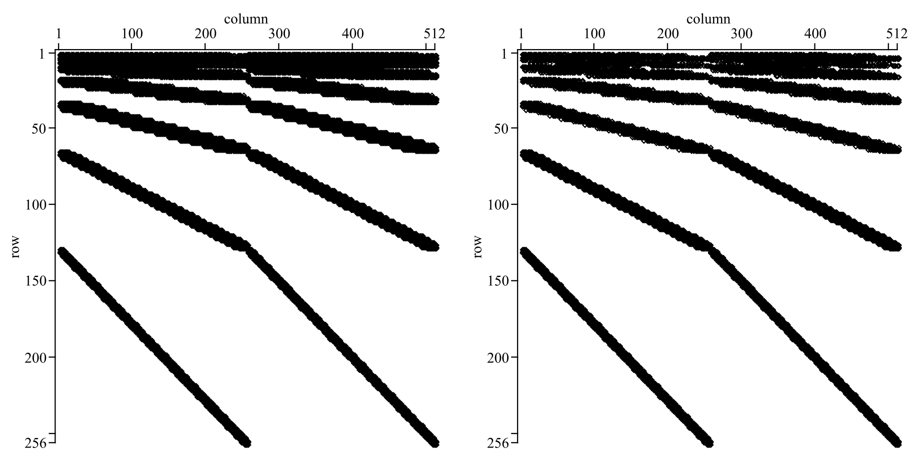

subject to the following dynamics

$$D_t^{\alpha} x(t) = tx(t) + u(t),$$

with initial condition

$$x(0) = 1.$$

In Table III, we compared the minimum of J obtained using the proposed method with Bernoulli basis [18]. In Figure 5, we demonstrate the approximation of the state $x(t)$ and

FIGURE 5. Approximate state and control variable for $\mathsf{J} = 7$ and $\alpha = 0.8, 0.9, .099, 1$, Example 2.

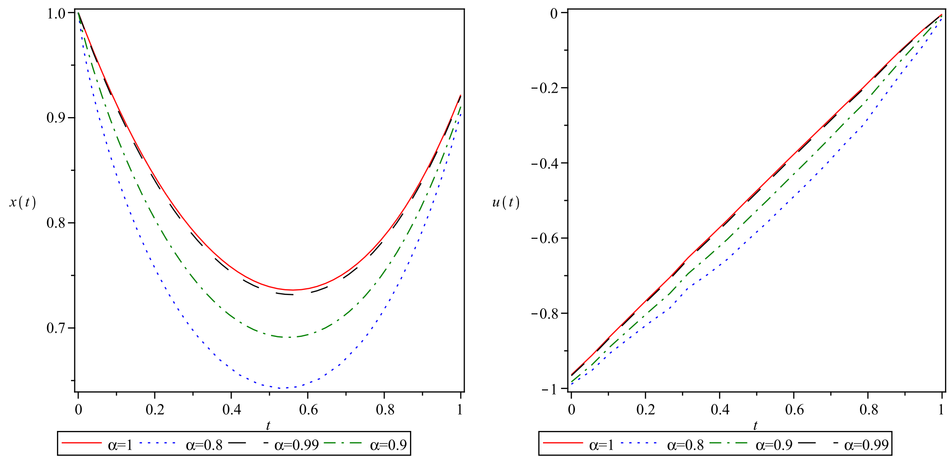

control $u(t)$ for different values of α. Also we show that when α tend to 1, the approximate solutions for both state and control variables tend to the exact solutions for $\alpha = 1$. The graphs of state variable $x(t)$ and control variable $u(t)$ for $\alpha = 0.8$ and $\mathsf{J} = 7,\ 8$ are plotted in Figure 6, It is obvious that with increase in the number of the biorthogonal wavelet basis, the approximate values of $x(t)$ and $u(t)$ converge to the exact solutions. Table IV, reports the sparsity and minimum value of J when $\alpha = 1$ for different values of thresholding parameter. Also Figure 7, shows the plot of the matrix elements for $\mathsf{J} = 7$ after thresolding.

Table III. Results for Example 2

Methods	J
Bernoulli basis [18]	
$\mathrm{M} = 5,\ \alpha = 0.8$	0.466978
$\mathrm{M} = 5,\ \alpha = 0.9$	0.475883
$\mathrm{M} = 5,\ \alpha = 0.99$	0.483463
$\mathrm{M} = 5,\ \alpha = 1$	0.484268
Biorthogonal multiwavelets	
$\mathsf{J} = 7,\ \alpha = 0.8$	0.466979
$\mathsf{J} = 7,\ \alpha = 0.9$	0.475887
$\mathsf{J} = 7,\ \alpha = 0.99$	0.483466
$\mathsf{J} = 7,\ \alpha = 1$	0.484270
$\mathsf{J} = 8,\ \alpha = 0.8$	0.466977
$\mathsf{J} = 8,\ \alpha = 0.9$	0.475883
$\mathsf{J} = 8,\ \alpha = 0.99$	0.483463
$\mathsf{J} = 8,\ \alpha = 1$	0.484268

Table IV. Estimated values for J, after thresholding, Example 2.

FIGURE 6. Comparison of state $x(t)$ (left) and $u(t)$ (right) for $\alpha = 0.8$ with $\mathsf{J} = 7,\ 8$, Example 2.

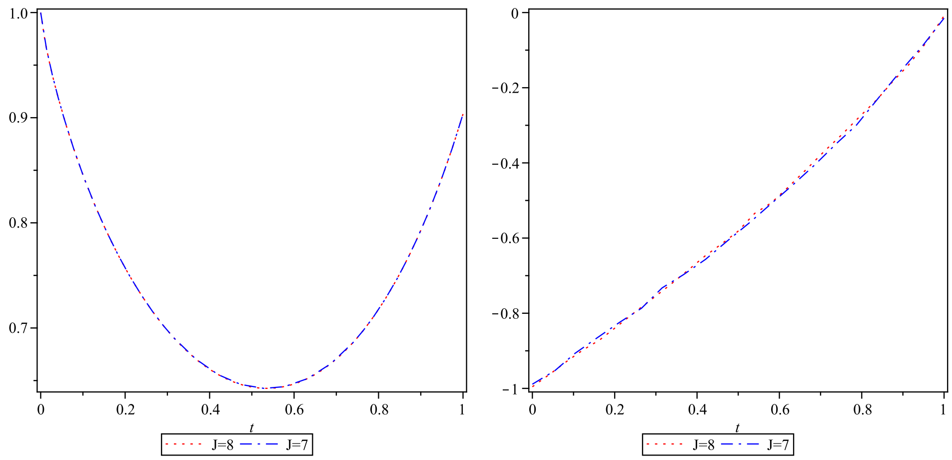

	Thresholding parameter (ε)	Sparsity (S_ε)	J
	0	0%	0.484278
$\mathsf{J} = 6$	10^{-4}	76.37%	0.484243
	10^{-3}	79.20%	0.483913
	10^{-2}	84.43%	0.485152
	0	0%	0.484270
$\mathsf{J} = 7$	10^{-4}	86.05%	0.484251
	10^{-3}	87.97%	0.483720
	10^{-2}	91.34%	0.483568

6. Conclusion

In this work the biorthogonal cubic Hermite spline multiwavelets are employed to solve a class of fractional optimal control problems. Considering the properties of these wavelets and using an approach based on the operational matrices of fractional integration and product and the Lagrange multiplier for constrained optimization, we convert the FOCPs to the solution of a system of algebraic equations. Using the spare structure of this system, the given problem is solved and memory times are reduced. Two numerical examples are given to observe the efficiency and applicability of the new method.

FIGURE 7. Plots of sparse matrices after thresholding with $\varepsilon = 10^{-5}$ (left) and $\varepsilon = 10^{-4}$ (right) for $\mathsf{J} = 7$, Example 2.

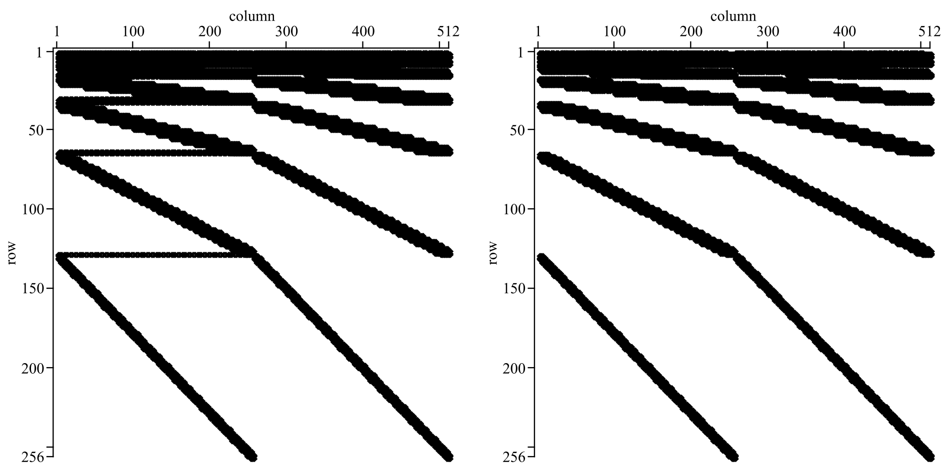

REFERENCES

[1] O. M. P. Agrawal, *General formulation for the numerical solution of optimal control problems*, Int. J. Control., *50* (1989), 627–638. DOI 10.1080/00207178908953385.

[2] O. M. P. Agrawal, *A general finite element formulation for fractional variational problems*, J. Math. Anal. Appl., *337* (2008), 1–12. DOI 10.1016/j.jmaa.2007.03.105.

[3] O. M. P. Agrawal, *Fractional variational calculus and transversality conditions*, J. Phys. A:Math. Gen., *39* (2006), 10375–10384. DOI 10.1088/0305-4470/39/33/008.

[4] O. M. P. Agrawal, *A general formulation and solution scheme for fractional optimal control problem*, Nonlinear Dynam., *38* (2004), 323–337. DOI 10.1007/s11071-004-3764-6.

[5] O. M. P. Agrawal, *A Hamiltonian formulation and a direct numerical scheme for fractional optimal control problems*, J. Vib. Control., *13* (2007), 1269–1281. DOI 10.1177/1077546307077467.

[6] O. M. P. Agrawal, *A formulation and numerical scheme for fractional optimal control problems*, J. Vib. Control., *14* (2008), 1291–1299. DOI 10.1177/1077546307087451.

[7] O. M. P. Agrawal, *A quadratic numerical scheme for fractional optimal control problems*, J. Dyn. Syst. Meas. Control., *130* (1) (2008), 011010 (6pages). DOI 10.1115/1.2814055.

[8] O. M. P. Agrawal, M. Mehedi Hasan and X. W. Tangpong, *A numerical scheme for a class of parametric problem of fractional variational calculus*, J. Comput. Nonlinear Dyn., *7* (2012), 021005–1. DOI 10.1115/1.4005464.

[9] R. Almedia and D. F. M. Torres, *Calculus of variations with fractional derivatives and fractional integrals*, Appl. Math. Lett., *22* (2009), 1816–1820. DOI 10.1016/j.aml.2009.07.002.

[10] R. Almedia, D. F. M. Torres, *Necessary and sufficient conditions for the fractional calculus of variations with Caputo derivatives*, Commun. Nonlinear Sci. Numer. Simul., *16* (2011), 1490–1500. DOI 10.1016/j.cnsns.2010.07.016.

[11] D. Baleanu, O. Defterli and O. M. P. Agrawal, *A central difference numerical scheme for fractional optimal control problems*, J. Vib. Control., *15* (2009), 547–597. DOI 10.1177/1077546308088565.

[12] G. Beylkin, R. Coifman and V.Rokhlin, *Fast wavelet transforms and numerical algorithms*, I, Commun. PureAppl. Math., *44* (1991), 141–183. DOI 10.1002/cpa.3160440202.

[13] C. K. Chui, Wavelets: *A Mathematical Tool for Signal Analysis*, SIAM, Philadelphia, PA, 1997.

[14] P. G. Ciarlet, M. H. Schultz and R. S. Varga, *Numerical methods of high-order accuracy for nonlinear boundary value problems I. One dimensional problems*, Numer. Math., *9* (1967) 294–430. DOI 10.1007/BF02165273.

[15] J. C. Goswami, A. K. Chan, and C. K. Chui, *On solving first-kind integral equations using wavelets on a bounded interval*, IEEE Trans. Antennas propagat., *43* (1995), 614–622. DOI 10.1109/8.387178.

[16] B. Han, *Approximation properties and construction of Hermite interpolants and biorthogonal multiwavelets*, J. Approx. Theory., *110* (2001), 18–53. DOI 10.1006/jath.2000.3545.

[17] B. Han and Q. Mo, *Multiwavelet frames from refinable function vectors*, Adv. Comput. Math., *18* (2003), 211–245. DOI 10.1023/A:1021360312348.

[18] E. Keshavarz, Y. Ordokhani and M. Razzaghi, *A numerical solution for fractional optimal control problems via Bernoulli polynomials*, J. Vib. Control., (2015), 1–15. DOI 10.1177/1077546314567181.

[19] A. A. Kilbas, H. M. Srivastava and J. J. Trujillo, *Theory and Applications of Fractional Differential Equations*, in:North-Holland Mathematics Studies., vol. *204*, Elsevier Science B.V, Amsterdam, 2006. DOI 10.1016/S0304-0208(06)80001-0.

[20] M. Lakestani, M. Dehghan and S. Irandoust-pakchin, *The construction of operational matrix of fractional derivatives using B-spline functions*, Commun. Nonlinear. Sci. Numer. Simulat., *17* (2012), 1149–1162. DOI 10.1016/j.cnsns.2011.07.018.

[21] A. Lotfi, S. A. Yousefi, *A numerical technique for solving a class of fractional variational problems*, J. Comput. Appl. Math., *237* (2013), 633–643. DOI 10.1016/j.cam.2012.08.005.

[22] A. Lotfi, M. Dehghan and S. A. Yousefi, *A numerical technique for solving fractional optimal control problems*, Computers and Mathematics with Applications *62* (2011), 1055–1067. DOI 10.1016/j.camwa.2011.03.044.

[23] A. Lotfi, S. A. Yousefi and M. Dehghan, *Numerical solution of a class of fractional optimal control problems via the Legendre orthonormal basis combined with the operational matrix and the Gauss quadrature rule*, Comput. Appl. Math., *250* (2013), 143–160. DOI 10.1016/j.cam.2013.03.003.

[24] K. B. Oldham and J. Spanier, *The Fractional Calculus*, NewYork: Academic Press (1974).

[25] I. Podlubny, *Fractional Differential Equations.* (1999) NewYork: Academic Press.

[26] C. Tricaud, Y. Q. Chen, *An approximation method for numerically solving fractional order optimal control problems of general form*, Comput. Math. Appl., *59* (2010), 1644–1655. DOI 10.1016/j.camwa.2009.08.006.

[27] S. A. Yousefi, A. Lotfi and M. Dehghan, *The use of a Legendre multiwavelet collocation method for solving the fractional optimal control problems*, J. Vib. Control., *13* (2011), 1–7. DOI 10.1177/1077546311399950.